Inorg. Chem. **2004**, *43*, 5860–5864

$Au_2(SeO_3)_2(SeO_4)$: Synthesis and Characterization of a New Noncentrosymmetric Selenite–Selenate

Mathias S. Wickleder,*,† Oliver BUchner,† Claudia Wickleder,† Sherif el Sheik,† Gunther Brunklaus,‡ and Hellmut Eckert‡

Universität zu Köln, Institut für Anorganische Chemie, Greinstrasse 6, 50939 Köln, Germany, and Westfälische Wilhelms-Universität Münster, Institut für Physikalische Chemie, Corrensstrasse 36, 48149 Münster, Germany

Received June 4, 2004

The reaction of elemental gold and selenic acid in Teflon-lined steel autoclaves leads to orange-yellow single crystals of $Au_2(SeO_3)_2(SeO_4)$ (orthorhombic, $Z = 4$, $Cmc2_1$ (No. 36), $a = 1689.1(3)$ pm, $b = 630.13(8)$ pm, $c = 832.7(1)$ pm, $V = 886.2(2)$ Å^3, $R_{all} = 0.0452$). In the crystal structure, Au^{3+} is surrounded by four oxygen atoms of just as many monodentate SeO_3^{2-} ions in a square planar manner. The linkage of the polyhedra leads to double chains $^1_\infty[Au_2(SeO_3)_2]^{2+}$ in the [001] direction which are connected to puckered layers by SeO_4^{2-} groups. The noncentrosymmetric space group could be proved by the observation of an SHG effect upon irridation at 1064 nm that shows an efficiency of about 43% compared to a KDP reference. Upon heating, $Au_2(SeO_3)_2(SeO_4)$ decomposes at about 370 °C in one step yielding elemental gold. The presence of selenite and selenate groups in the compounds is also obvious from the IR and Raman spectra which show the characteristic bands of both species. Furthermore, solid-state NMR spectra reveal the different surroundings of the selenium atoms in the compound.

Introduction

It has been well-known for nearly 200 years that concentrated selenic acid can dissolve elemental gold, and Mitscherlich was the first to report this reaction.[1] Later, Lenher repeated the reaction and claimed that the yellow compound he obtained was $Au_2(SeO_4)_3$.[2] Coldwell and Eddy investigated the reaction in more detail in 1949 and pointed out that $Au_2(SeO_4)_3$ may be used in glass coloring processes.[3] However, roughly 20 years ago it was shown that in fact selenites form during the dissolution of elemental gold in selenic acid and have, depending on the specific conditions, the different compositions $Au_2(SeO_3)_2O$ and $Au_2(SeO_3)_2(Se_2O_5)$.[4] On the other hand, selenates can be prepared by the reaction of selenic acid and $Au(OH)_3$ according to Donova and Šiftar.[5] Unfortunately, the latter have not been characterized. In the course of our investigations on gold compounds with complex oxoanions,[6] we have now reinvestigated the system Au/H_2SeO_4 and were able to synthesize a new gold compound, $Au_2(SeO_3)_2(SeO_4)$, in single crystalline form. This compound is of special interest for two reasons: On one hand, it is mixed valent with respect to the oxidation state of selenium and thus extends the still very limited group of mixed valent selenates which contains up to now for example the mineral schmiederit, $Pb_2Cu_2(OH)_4(SeO_3)(SeO_4)$,[7] the compounds $Li_2Cu_3(SeO_3)_2(SeO_4)_2$,[8] $Er_2(SeO_3)_2(SeO_4)\cdot 2H_2O$,[9] $NaSm(SeO_3)(SeO_4)$,[10] $Pr_4F_6(SeO_3)_2(SeO_4)$,[10] $Hg_3(SeO_3)_2(SeO_4)$,[11] and the acidic species $Na_2SeO_4\cdot H_2SeO_3\cdot H_2O$,[12] $Fe(HSeO_3)(SeO_4)\cdot H_2O$,[13] and $La(HSeO_3)$-

* To whom correspondence should be addressed. E-mail: mathias.wickleder@uni-koeln.de.
† Universität zu Köln, Institut für Anorganische Chemie.
‡ Westfälische Wilhelms-Universität Münster, Institut für Physikalische Chemie.

(1) Mitscherlich, E. *Pogg. Ann.* **1827**, *9*, 623.
(2) Lenher, V. *J. Am. Chem. Soc.* **1902**, *24*, 354.
(3) Coldwell, W. E.; Eddy, L. P. *J. Am. Chem. Soc.* **1949**, *71*, 2247.
(4) (a) Jones, P. G.; Sheldrick, G. M.; Schwarzmann, E.; Vielmäder, A. *Z. Naturforsch.* **1983**, *38b*, 10. (b) Jones, P. G.; Schwarzmann, E.; Sheldrick, G. M.; Timpe, H. *Z. Naturforsch.* **1981**, *36b*, 1050.
(5) Donova, I.; Šiftar, J. *Thermochim. Acta* **1994**, *244*, 131.
(6) (a) Wickleder, M. S. *Z. Anorg. Allg. Chem.* **2001**, *627*, 2112. Wickleder, M. S.; Büchner, O. *Z. Kristallogr.* **2003**, (Suppl. 20), 157. Wickleder, M. S.; Büchner, O. *Z. Naturforsch.* **2001**, *56b*, 1340. Wickleder, M. S.; Esser, K. *Z. Anorg. Allg. Chem.* **2002**, *628*, 911.
(7) Effenberger, H. *Mineral. Petrol.* **1987**, *36*, 3.
(8) Giester, G. *Monatsh. Chem.* **1989**, *120*, 661.
(9) Morris, R. E.; Wilkinson, A. P.; Cheetham, A. K. *Inorg. Chem.* **1992**, *31*, 4774.
(10) Krügermann, I.; Wickleder, M. S. *Z. Anorg. Allg. Chem.* **2002**, *628*, 147.
(11) Weil, M.; Kolitsch, U. *Acta Crystallogr.* **2002**, *C58*, 47.

10.1021/ic049270z CCC: $27.50
Published on Web 08/17/2004

Table 1. $Au_2(SeO_3)_2(SeO_4)$ Crystallographic Data and Their Determination

lattice parameters (single crystal/powder data)	$a = 1689.1(3)/1691.2(3)$ pm, $b = 630.13(8)/630.55(9)$ pm, $c = 832.7(1)/832.6(2)$ pm
cell volume	886.2(2)/887.8(2) Å^3
no. of formula units	4
cryst syst	orthorhombic
space group	$Cmc2_1$ (No. 36)
measuring device	Stoe IPDS I
radiation	Mo Kα (graphite monochromatized, $\lambda = 71.07$ pm)
temp	20 °C
θ range	$5° < 2\theta < 56°$
index range	$-22 \le h \le 22$ $-8 \le k \le 8$ $-10 \le l \le 10$
rotation angle; φ increment	$0° < \varphi < 200°$; 2°
no. of exposures	100
exposure time	5 min
detector distance	60
data corrections	polarization and Lorentz factors
absorption correction	numerical
μ	454.3 cm^{-1}
measured reflections	5054
unique reflections	1087
with $I_0 > 2\sigma(I)$	905
no. of variables	74
R_{int}	0.0800
structure determinations	SHELXS-86 and SHELXL-93
scattering factors	ref 35
extinction coefficient	0.0019(2)
GOF (obs/all)	1.044/0.986
R1; wR2 ($I_0 > 2\sigma(I)$)	0.0362; 0.0838
R1; wR2 (all data)	0.0452; 0.0873
Flack-x	−0.04(3)
min/max electron density/e Å^{-3}	−2.565/3.147
depository number	414094

$(SeO_4)\cdot 2H_2O$.[14] On the other hand, $Au_2(SeO_3)_2(SeO_4)$ crystallizes with a noncentrosymmetric space group. According to a recent review, noncentrosymmetric oxides play an important role as second harmonic generation (SHG) materials,[15] and especially, Se^{4+}-containing compounds have attracted considerable interest owing to the lone electron pair that enhances the polarizability.[16−18] With respect to these findings also for $Au_2(SeO_3)_2(SeO_4)$, a remarkable SHG effect can be expected.

Experimental Section

Synthesis. A few pieces (1 g) of elemental gold (Degussa) and 10 mL of concentrated selenic acid were placed in a Teflon-lined steel autoclave (Parr Instruments, V = 23 mL) and heated to 250 °C in 10 h, followed by slow cooling at 5 °C/h. The synthesis of the selenic acid was carried out starting from SeO_2 (Acros, 99.9%) and H_2O_2 (30%, Merck, p.a.) according to the procedure given in ref 19. The reaction product contained some unreacted gold and yellow-orange plate shaped single crystals (80% with respect to the initial gold). They were washed with water and dried in air.

Table 2. $Au_2(SeO_3)_2(SeO_4)$ Atomic Positions and Equivalent Displacement Parameters[a]

atom	Wyckoff	x/a	y/b	z/c	$U_{eq} \times 10^{-1}$/pm^2
Au	8*b*	0.65956(3)	0.97575(8)	0.68380(1)	16.9(2)
Se1	8*b*	0.8386(1)	0.9677(3)	0.8042(2)	18.2(4)
O11	8*b*	0.8457(7)	0.8397(18)	0.1604(18	24(3)
O12	8*b*	0.6697(8)	0.2859(21)	0.6496(14)	24(3)
O13	8*b*	0.7389(6)	0.9783(19)	0.8627(11)	16(2)
Se2	4*a*	0	0.6405(4)	0.5325(3)	19.5(5)
O21	4*a*	0	0.1976(40)	0.8797(24)	35(4)
O22	8*b*	0.5801(7)	0.9700(21)	0.5065(15)	25(2)
O23	4*a*	0	0.7378(34)	0.7127(25)	38(6)

[a] $U_{eq} = {}^1/_3[U_{11} + U_{22} + U_{33}]$.

Table 3. Selected Distances (pm) and Angles (deg) for $Au_2(SeO_3)_2(SeO_4)$

Se1−O12		198.2(13)	O12−Au−O22		88.3(5)
Se2−O22		199.5(12)	O12−Au−O11		165.9(6)
Au−O11		199.9(12)	O12−Au−O13		92.4(5)
Se1−O13		200.4(10)	O22−Au−O11		83.1(5)
			O22−Au−O13		179.3(5)
			O11−Au−O13		96.3(5)
Se1−O11		170.9(13)	O11−Se1−O12		87.4(7)
Se1−O12		172.9(12)	O11−Se1−O13		103.6(5)
Se1−O13		175.6(11)	O12−Se1−O13		98.8(6)
Se2−O23		162.0(20)	O23−Se2−O21		119.1(12)
Se2−O21		163.1(20)	O23−Se2−O22	(2×)	110.4(6)
Se2−O22	(2×)	174.1(13)	O21−Se2−O22	(2×)	106.8(7)
			O22−Se2−O22		102.0(9)

X-ray Crystallography. For the structure determination, some crystals were sealed in glass capillaries and checked for their quality using an image plate diffractometer (IPDS I). With the same device, the reflection intensities of the best specimen were collected. The structure solution and refinement was successful in space group $Cmc2_1$ using the programs SHELXS86 and SHELXL93, respectively.[20,21] A numerical absorption correction was applied to the data with the help of the programs X-RED and X-SHAPE.[22,23] Details of the data collection and the cyrstallographic parameters are summarized in Tables 1−3. For the powder diffraction measurement, the fine powdered substance was placed on a flat sample holder, and reflections were detected in the range 5−90° using the diffractometer STADI P equipped with a PSD (Fa. Stoe). Lattice parameter refinement was performed with the help of the diffractometer's software.[24] The refined data are given in Table 1 additionally.

Vibrational Spectroscopy. The IR spectra were taken on a sample prepared in KBr (MIR) and polyethylene (FIR) pellets with the spectrometer IFS 66v/s (BRUKER). The same spectrometer in combination with a Raman equipment (FRA 166/S) was used for the measurement of the Raman spectrum with a resolution of 2 cm^{-1} and 1064 nm radiation of a Nd:YAG laser as excitation scource. Observed bands and their assignment are collected in Table 4.

Thermal Analysis. For the investigation of the thermal behavior, 20 mg of the compound was placed in a corundum container which

(12) Baran, J.; Lis, T.; Marchewka, M.; Ratajczak, H. *J. Mol. Struct.* **1991**, *250*, 13.
(13) Giester, G. *Monatsh. Chem.* **1992**, *123*, 957.
(14) Harrison, W. T. A.; Zhang, Z. *Eur. J. Solid State Inorg. Chem.* **1997**, *34*, 599.
(15) Halasyamani, P. S.; Poeppelmeier, K. R. *Chem. Mater.* **1998**, *10*, 2753.
(16) Ok, K. M.; Halasyamani, P. S. *Chem. Mater.* **2002**, *14*, 2360.
(17) Berdonosov, P. S.; Stefanovitch, S. Yu.; Dolgikh, V. A. *J. Solid State Chem.* **2000**, *149*, 236.
(18) Porter, Y.; Halasyamani, P. S. *J. Solid State Chem.* **2003**, *174*, 441.
(19) *Handbuch der Präparativen Anorganischen Chemie, Bd I*; Bauer, G., Ed.; F. Enke Verlag: Stuttgart, 1975.
(20) Sheldrick, G. M. *SHELXS86, Programme zur Röntgenstrukturanalyse*; University of Göttingen: Göttingen, Germany, 1986.
(21) Sheldrick, G. M. *SHELXL93, Program for the Refinement of Crystal Structures*; University of Göttingen: Göttingen, Germany, 1993.
(22) *X-RED 1.07, Data Reduction for STADI4 and IPDS*; Stoe & Cie: Darmstadt, Germany, 1996.
(23) *X-SHAPE 1.01, Crystal Optimisation for Numerical Absorption Correction*; Stoe & Cie: Darmstadt, Germany, 1996.
(24) *VISUAL X^{POW} 3.01, software package for the STOE powder diffraction system*; Stoe & Cie: Darmstadt, Germany, 1996.

Table 4. IR and Raman Data (cm^{-1}) for the Anions in $Au_2(SeO_3)_2(SeO_4)$

free ion	mode	observed IR	observed Raman
	SeO_3^{2-} (C_{3v})		
$\nu_1(A_1)$, 810	ν_s (SeO_2)	806	
$\nu_2(A_1)$, 425	δ_s (SeO_3)	451, 428	
$\nu_3(E)$, 740	ν_{as} (SeO_2)	760, 686	772, 687
$\nu_4(E)$, 372	δ_{as} (SeO_3)	382	
	SeO_4^{2-} (T_d)		
$\nu_1(A_1)$, 837	ν_s (SeO_2)	858	853
$\nu_2(A_1)$, 345	δ_s (SeO_4)	362	340
$\nu_3(F_2)$, 873	ν_{as} (SeO_2)	956, 895, 875	965, 897
$\nu_4(F_2)$, 413	δ_{as} (SeO_4)	392	

was heated (10 K/min) up to 500 °C under flowing argon using the thermoanalyzer STA 409 (NETZSCH). The data were processed with the software of the analyzer.[25]

Second Harmonic Generation. The measurements of the SHG effect were done according to the technique described by Kurtz and Perry.[26] As a reference substance, potassium dihydrogen phosphate (KDP) was used. Because the intensity of the second harmonic radiation depends on the particle size, carefully ground powder samples of both compounds are used. Thin layers (about 0.5 mm) of the powders were placed on a microscope slide and fixed with transparent tape. Irridiation was achieved by the fundamental radiation of a pulsed Nd:YAG laser (GCR 11, Spectra Physics, pulse duration 8 ns, 10 Hz). To avoid destruction of the compound, the laser power was reduced to about 50 mJ/pulse. To ensure a nearly constant power which is important for the comparison of the SHG intensities of both compounds, a small part of the laser beam was coupled out and monitored by an oscilloscope. The main part was slightly focused on the sample. The originating radiation was focused on the entrance slit of a monochromator and detected by a photomultiplier (Hamamatsu, R2949). Fortunately, the absorption of $Au_2(SeO_3)_2(SeO_4)$ starts at higher energy than the frequency doubled 532 nm radiation, so that no excitation due to the second harmonic radiation occurred.

Solid-State NMR Spectroscopy. The ^{77}Se solid-state NMR spectrum was obtained on a Bruker DSX-400 spectrometer equipped with a 4 mm magic angle spinning (MAS) probe, operated at a spinning frequency of 12 kHz. There were 1200 transients accumulated using 90° pulses of 2.5 μs length and relaxation delays of 120 s (overall experimental time 40 h). Experiments carried out with different relaxation delays resulted in comparable intensity ratios of the peaks observed. A saturated aqueous solution of selenious acid (H_2SeO_3) was used as external reference. On the basis of the measured intensity distribution of the MAS rotation sidebands, the anisotropic chemical shift parameters were extracted using the program DMFIT. For the chemical shift anisotropy parameter, the definition $\Delta\sigma = \sigma_{33}\text{-}\sigma_{iso}$ was used, where $|\sigma_{33} - \sigma_{iso}| > |\sigma_{11} - \sigma_{iso}| > |\sigma_{22} - \sigma_{iso}|$.

Results and Discussion

Crystal Structure. In the crystal structure of $Au_2(SeO_3)_2(SeO_4)$, the Au^{3+} ions are surrounded by four oxygen atoms in a square planar manner. The distances within the $[AuO_4]$ square are nearly equal and about 200 pm (Table 3). The angles ∠O−Au−O show significant deviations from 90° with the respective lowest and largest values being 83.1(5)° and 96.3(5)°. Three oxygen atoms (O11−O13) in the $[AuO_4]$ unit belong to monodentate selenite groups, the fourth (O22) to a monodentate selenate ion. The SeO_3^{2-} ions are connected to two further Au^{3+} ions in a way that strands are formed according to $^1_\infty[Au(SeO_3)_{3/3}]^+$ and are running along the [010] direction (Figure 1). The distances and angles within the SeO_3^{2-} ion range from 170.9(13) to 175.6(11) pm and from 87.4(7)° to 103.6(5)°, respectively, indicating severe distortion of the typical pyramidal shape of the anion. Especially, the angle at 87.4(7)° is quite small compared to the typical values which range usually from 97° to 104°.[27] On the other hand, the same observation has been made for the gold selenites known so far.[4] The connection of the $^1_\infty[Au(SeO_3)_{3/3}]^+$ chains by SeO_4^{2-} ions leads to infinite puckered layers $^2_\infty[Au(SeO_3)_{3/3}(SeO_4)_{1/2}]$ parallel to (001) as can be seen from Figure 2. The sheets are stacked in the same orientation with respect to each other so that only a 2_1 screw axis is present in the [001] direction causing the noncentrosymmetric space group. The layers are held together by weak contacts between Au^{3+} ions and the oxygen atoms O13 (Figure 2). Although the respective distance is quite long (300.5(11) pm), it is remarkable that the correlated distance Se−O13 is the longest within the SeO_3^{2-} ion. The two oxygen atoms (O22) of the selenate ion which are involved in the linkage of the $^1_\infty[Au(SeO_3)_{3/3}]^+$ chains are related by a mirror plane because the Se2 atom is located on a special site (4*a*) of the space group *Cmc*2_1. The distance Se2−O22 is found to be 174.1(13) pm and thus is very long compared to the distances of the noncoordinating oxygen atoms which are 162.0(20) and 163.1(20) pm, respectively. The same significant bond length differentiation has been observed in $RbAu(SeO_4)_2$ which is the only structurally characterized gold selenate so far and which shows also two oxygen atoms of the SeO_4^{2-} ion attached to Au^{3+}.[28] Furthermore, the observed distances within the SeO_4^{2-} ion

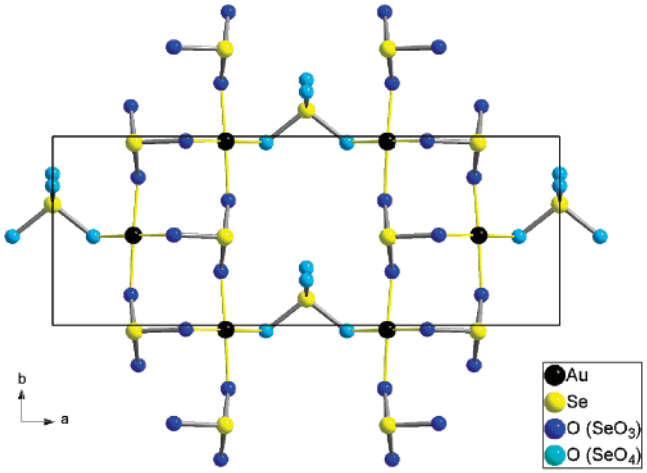

Figure 1. Crystal structure of $Au_2(SeO_3)_2(SeO_4)$. The Au^{3+} ions are connected by selenite ions to strands according to $^1_\infty[Au(SeO_3)_{3/3}]^+$ which are further connected by selenate groups to puckered layers $^2_\infty[Au(SeO_3)_{3/3}(SeO_4)_{1/2}]$.

(25) *Thermal analysis for the analyzer STA 409, version 3.1*; NETZSCH GmbH: Selb, Germany, 1996.
(26) Kurtz, S. K.; Perry, T. T. *J. Appl. Phys.* **1968**, *39*, 3798.
(27) Koskenlinna, M. Ph.D. Thesis, Helsinki University of Technology, Espoo, Finland, 1996.
(28) Büchner, O.; Wickleder, M. S. *Z. Anorg. Allg. Chem.*, in press.

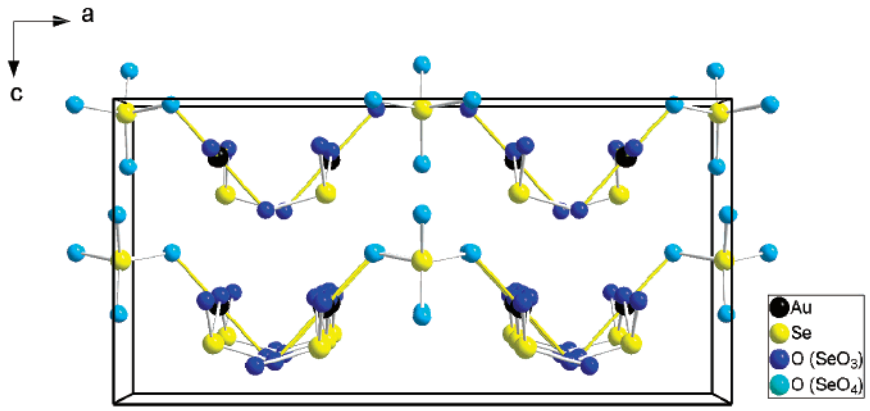

Figure 2. Perspective view of the crystal structure of $Au_2(SeO_3)_2(SeO_4)$ along [010].

are comparable with the data reported for H_2SeO_4.[29] Thus, it can be assumed that the short distances correspond to Se−O double bonds and the longer ones to Se−O single bonds. Judged from the angles ∠O−Se−O which range from 102.0(9)° to 119.1(12)°, the tetrahedral shape of the anion is strongly distorted. As suggested by the VSEPR model, the large angle occurs between the double bonded oxygen atoms.[30]

Vibrational Spectroscopy. The presence of selenite and selenate ions in the structure of $Au_2(SeO_3)_2(SeO_4)$ can also be seen from the IR and Raman spectra. According to their respective site symmetries in the lattice, the symmetry of the anions has changed from C_{3v} to C_1 (SeO_3^{2-}) and from T_d to C_s (SeO_4^{2-}) with respect to the free species. Thus, six normal modes can be expected for the SeO_3^{2-} ion and nine for SeO_4^{2-} if a factor group splitting is neglected.[31] The observed bands for the anions are summarized in Table 4 and match pretty well the typical values which have been found for various selenites and selenates.[32] Besides the vibrations of the anions, two prominent bands occur in the IR spectrum at 586 and 537 cm^{-1}, and three bands at 585, 539, and 517 cm^{-1} are found in the Raman spectrum. According to the findings for Au_2O_3, these transitions can be attributed to vibrations within the [AuO_4] unit.[33]

Solid-State NMR Spectroscopy. Figure 3 shows the ^{77}Se MAS NMR spectrum of this compound. Two MAS sideband patterns centered at 87.9 and −235.5 ppm can be discerned, having an overall intensity ratio of approximately 2:1. On the basis of this intensity ratio, the 87.9 ppm resonance must be assigned to the selenite species and the −235.5 ppm signal to the selenate species. This assignment is consistent with the general observation that the higher coordinated species appear at lower resonance frequencies. Spinning sidebands of considerable intensity reflect the fact that the MAS rotor frequency is insufficient to remove the chemical shielding anisotropies (csa) associated with both selenium species. Simulations of the MAS sideband intensity profiles, using the DMFIT software, indicate that the shielding tensors are approximately axially symmetric for both selenium sites, with a significantly larger anisotropy observed for the SeO_4^{2-} group. Unfortunately, the spin−lattice relaxation times are excessively long, resulting in a rather low signal-to-noise ratio, which precludes the observation of lower intensity spinning sidebands. Therefore, Figure 3 (bottom trace) includes also a predicted sideband pattern based on the parameters used to simulate the experimental spectrum. The large csa evident for the selenate group might seem surprising in view of the fact that an anisotropy of zero would be expected for an ideal selenate ion with T_d point symmetry. Inspection of Table 3 reveals, however, that in $Au_2(SeO_3)_2(SeO_4)$ the selenate ion is highly distorted: the Se−O bond lengths vary from 162.0(20) to 174.1(13) pm, and the overall spread of tetrahedral bond angles is approximately 17°. The large deviation of the selenate group from tetrahedral symmetry also manifests itself in the vibrational spectra, where the A_1 mode associated with the Se−O stretching motion deviates strongly from that predicted for an ideal tetrahedral species.

Second Harmonic Generation. If a powder sample of $Au_2(SeO_3)_2(SeO_4)$ is irradiated by the infrared fundamental beam of the Nd:YAG laser (1064 nm), bright green radiation can be observed by eye. For proof, a respective spectrum in the range 400−800 nm was taken. In this region, only one peak with a maximum at 532 nm was observed as expected due to the frequency doubling process while the width was determined by the resolution of the monochromator. For an assessment of the SHG efficiency of $Au_2(SeO_3)_2(SeO_4)$, a spectrum of KDP was recorded using the same equipment with identical settings. KDP is a frequently used noncentrosymmetrical material with a large SHG effect (type I, $d_{eff} = 0.2553$; type II, $d_{eff} = 0.3464$ for $\lambda = 1064$ nm[34]). The integration of the peaks of both spectra yielded a efficiency

(29) Erfany-Far, H.; Fuess, H.; Gregson, D. *Acta Crystallogr.* **1987**, *C43*, 395.
(30) Gillespie, R. J.; Nyholm, R. S. *Q. Rev., Chem. Soc.* **1957**, *11*, 339.
(31) (a) Weidlein, J.; Müller, U.; Dehnicke, K. *Schwingungsspektroskopie*; Thieme: Stuttgart, 1988. (b) Siebert, H. *Anwendung der Schwingungsspektroskopie in der Anorganischen Chemie*; Springer: Berlin, 1966.
(32) (a) Sathianandan, K.; McCory, L. D.; Margrave, J. L. *Spectrochim. Acta* **1964**, *20*, 957. (b) Verma, V. P. *Thermochim. Acta* **1999**, *327*, 63 and references therein.
(33) (a) Schwarzmann, E.; Fellwock, E. *Z. Naturforsch.* **1971**, *26b*, 1469. (b) Jansen, M.; Mudring, A. V. In *Gold, Progress in Chemistry, Biochemistry and Technology*; Schmidbaur, H., Ed.; John Wiley & Sons: Chichester, 1999; p 753.
(34) Eimerl, D. *Ferroelectrics* **1987**, *72*, 95.
(35) *International Tables for Crystallography, Vol. C*; Hahn, Th., Ed.; D. Reidel Publishing Company: Dordrecht, 1983.

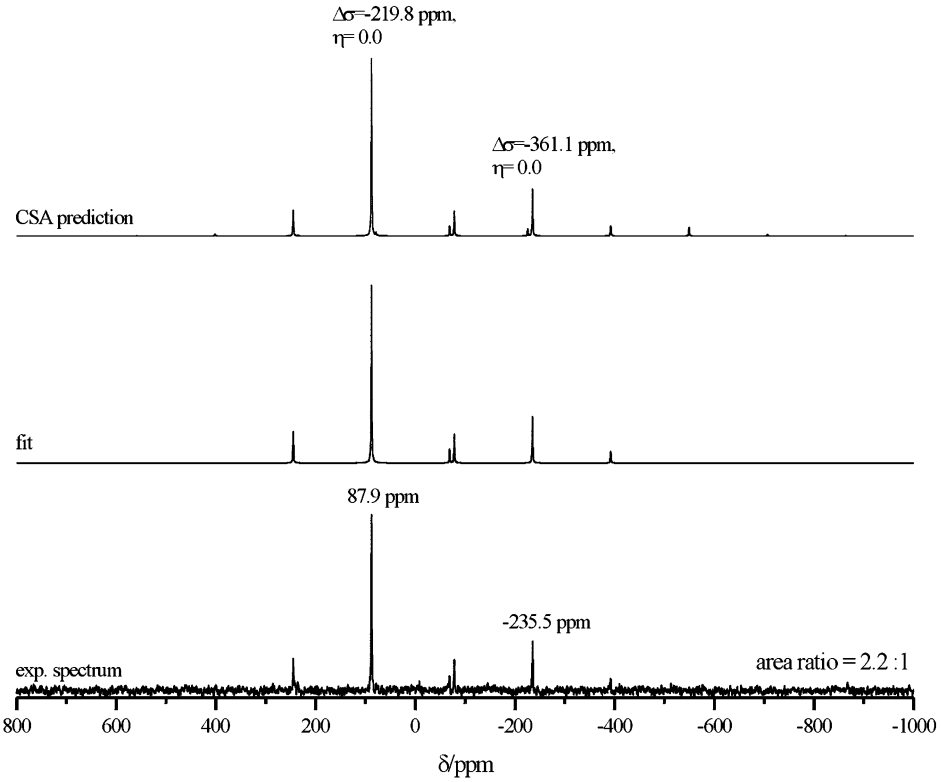

Figure 3. ^{77}Se MAS NMR spectroscopy of $Au_2(SeO_3)_2(SeO_4)$. The bottom trace shows the experimental spectrum. MAS centerbands have been labeled with the corresponding isotropic chemical shifts; all other peaks not labeled are MAS rotation sidebands. The middle trace shows the best fit of the MAS sideband pattern corresponding to the anisotropic chemical shift parameters displayed together with the top trace, which shows the theoretical prediction.

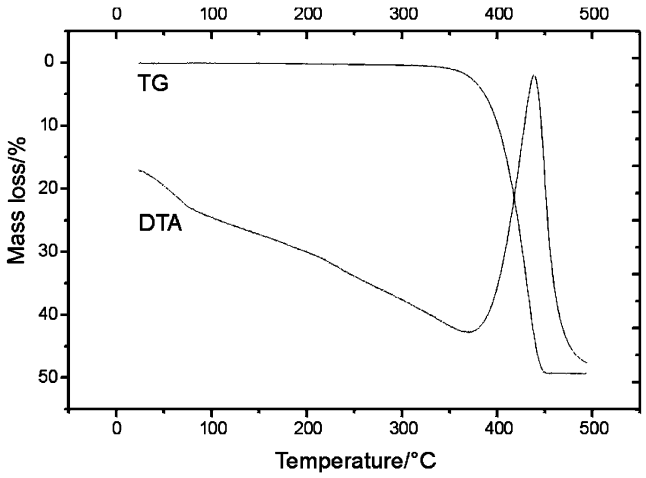

Figure 4. DTA/TG diagram of the thermal decomposition of $Au_2(SeO_3)_2(SeO_4)$.

of 43% for $Au_2(SeO_3)_2(SeO_4)$ relative to those of KDP. This is only a rough estimation, because the efficiency depends on the particle size, and on the other hand, the intensity depends on the angle between the direction of the incident radiation and the detector.[26] Therefore, for more quantitative investigations of the SHG efficiency an integration sphere for detection must be used. More detailed investigations are currently in progress.

Thermal Decomposition. The thermal decomposition of $Au_2(SeO_3)_2(SeO_4)$ follows a one-step mechanism, and with respect to the observed mass loss, it leads to elemental gold (Figure 4). The onset of the decomposition is 373 °C, and the reaction is complete at 481 °C. The maximum of the peak is at 438 °C, which is significantly higher than the temperatures which have been observed for the decomposition of the ternary selenates $M[Au(SeO_4)_2]$ (M = K−Cs).[5]

Acknowledgment. This work has been supported by the Deutsche Forschungsgemeinschaft (Graduiertenkolleg 549). Furthermore, we thank Prof. Gerd Meyer for generous support. G.B. and O.B. acknowledge support by the Fonds der Chemischen Industrie for doctoral stipends.

Supporting Information Available: Crystallographic data in CIF format. This material is available free of charge via the Internet at http://pubs.acs.org. Furthermore, the data have been deposited with the Fachinformationszentrum Karlsruhe, D-76344 Eggenstein-Leopoldshafen (crysdata@FIZ-Karlsruhe.de), and are available on quoting the deposition number given in Table 1.

IC049270Z